

## Use of Ring Sample for High-Pressure Torsion and Microstructural Evolution with Equivalent Strain

Ito, Yuki

Department of Materials Science and Engineering, Faculty of Engineering, Kyushu University

Harai, Yosuke

Department of Materials Science and Engineering, Faculty of Engineering, Kyushu University

Fujioka, Tadayoshi

Department of Materials Science and Engineering, Faculty of Engineering, Kyushu University

Edalati, Kaveh

Department of Materials Science and Engineering, Faculty of Engineering, Kyushu University

他

<https://hdl.handle.net/2324/26386>

---

出版情報 : Materials Science Forum. 584/586, pp.191-196, 2008-06. Trans Tech Publications  
バージョン :  
権利関係 : (C) (2008) Trans Tech Publications, Switzerland

## Use of Ring Sample for High-Pressure Torsion and Microstructural Evolution with Equivalent Strain

Yuki Ito, Yosuke Harai, Tadayoshi Fujioka, Kaveh Edalati<sup>a</sup> and Zenji Horita<sup>b</sup>

Department of Materials Science and Engineering, Faculty of Engineering

Kyushu University, Fukuoka 819-0395, Japan

<sup>a</sup>[kaveh.edalati@zaiko6.zaiko.kyushu-u.ac.jp](mailto:kaveh.edalati@zaiko6.zaiko.kyushu-u.ac.jp), <sup>b</sup>[horita@Zaiko0.kyushu-u.ac.jp](mailto:horita@Zaiko0.kyushu-u.ac.jp)

**Keywords:** hardness, high-pressure torsion, homogeneity, Al, Cu, equivalent strain

**Abstract.** This study introduces a process of high-pressure torsion (HPT) using ring samples and compares with the results of conventional disk HPT. Both types of HPT were conducted at room temperature on pure Al and pure Cu. The microhardness was measured along the diameters of the disks and rings. Microstructures were examined using transmission electron microscopy. When hardness values were plotted against equivalent strain, all data points fell on a single line for each material. There was a hardness maximum for pure Al but no such a maximum was present in pure Cu. In pure Al, many dislocations were visible within grains up to the equivalent strain corresponding to the hardness maximum but beyond this strain, grains with low dislocation density appear. All materials exhibited steady state where the hardness remains constant with respect to imposed equivalent strain. This study concludes that use of ring samples is effective as an alternative to the disk samples.

### Introduction

High Pressure Torsion (HPT) is a typical process of severe plastic deformation producing ultrafine grains in metallic materials. Conventionally, a sample for the HPT process is used in a form of disk [1] and occasionally, in a form of cylinder [2]. For both cases, however, the shear strain is introduced in proportion to the distance from the center so that an inhomogeneous microstructure develops along the diameter. To circumvent this microstructural inhomogeneity, it was suggested to use inner hollow samples [3] and in practice it was shown that a ring form is applicable in the HPT process [4,5]. Recently, ring samples of pure Al were used with a simple extension of the facility for a disk sample and it was demonstrated that homogeneous microstructure is attained throughout the ring [6]. Furthermore, an advantage of using the ring geometry was shown such that the ring diameter can be increased by the amount of the inner hollow region so that it is possible to introduce more strain in the ring sample if the rotation angle is the same or less rotation is required if the same strain is imposed. This advantage was demonstrated by plotting the hardness as a function of equivalent strain, where all hardness data fell on a single unique line regardless of the use of disk samples or ring samples.

In this study, pure Al and pure Cu are processed with HPT using both disk and ring samples and it is examined if the hardness variation is expressed with such a single unique function of equivalent strain for each of the metals. Furthermore, microstructural evolution is examined and the mechanism for grain refinement is discussed in terms of stacking fault energy.

### Experimental procedures

HPT samples were prepared from high purity Al (99.99%) and Cu (99.99%). They have 10 mm diameter for disks and outer diameters of 20 or 30 mm with 3 mm width for rings. Figure 1 shows the sample configurations used in this study. All samples had a thickness of 0.8 mm. The samples were annealed for 1 hour at 773 K and 873 K for the Al and Cu, respectively.

HPT was conducted using the facilities as schematically illustrated in Fig.2 for (a) the disk sample and (b) for the ring sample. The facilities consist of upper and lower anvils having a shallow hole of

10mm diameter and 0.25mm depth at the centers for the disk samples and having a shallow circular groove with the inner and outer diameters of 14 mm and 20 mm or 24 mm and 30 mm with the groove depth of 0.25 mm around the center for the ring samples. Each sample was placed on the hole or on the groove and the lower anvil was rotated with respect to the upper anvil at room temperature with a rotation speed of 1 rpm for pure Al under a pressure of 1 GPa and with a rotation speed of 0.5 rpm under a pressure of 2 GPa for pure Cu. The rotation was terminated after a revolution of either 1/8, 1/4, 1/2, 1, 2, 4 or 10.

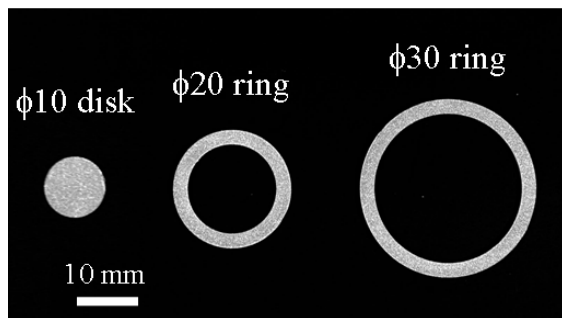


Fig. 1 Appearance of disk and ring samples .

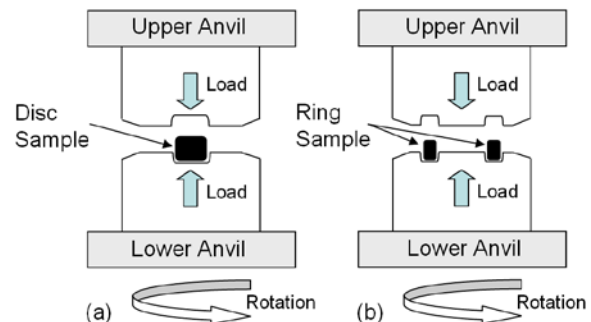


Fig. 2 Schematic illustration of (a) disk HPT and (b) ring HPT.

The disks and ring samples subjected to HPT were polished to a mirror-like surface and thus the Vickers microhardness was measured along the radii from the center to edge at 12 different radial directions for the disk and ring samples. The average was taken from the 12 measurements at the same distance from the center of disks or rings. Loads of 50 and 200 g were applied for 15 seconds in pure Al pure Cu, respectively, using an Akashi MVK-E3 testing machine.

Transmission electron microscopy (TEM) was performed for ring samples. Disks with 3 mm in diameter were cut from the ring and ground mechanically to a thickness of 0.15 mm. They were further thinned with a twin-jet electro-chemical polisher using a solution of 10%  $\text{HClO}_4$ , 20%  $\text{C}_3\text{H}_8\text{O}_3$  and 70%  $\text{C}_2\text{H}_5\text{OH}$  at 273 K for pure Al and using a solution of 10%  $\text{HNO}_3$ , 20%  $\text{C}_3\text{H}_5(\text{OH})_3$  and 70%  $\text{C}_2\text{H}_5\text{OH}$  at 273 K for pure Cu. A Hitachi H-8100 transmission electron microscope was operated at 200 kV for microstructural observation.

## Results

Figures 3 and 4 plot Vickers microhardness as a function of distance from the center of disks and rings after revolutions of 1/8 to 1 under a pressure of 1 GPa for Al and after revolutions of 1/8 to 10 under a pressure of 2 GPa for Cu, respectively. For both Al and Cu, the hardness variation strongly depends on the extent of revolution, and further the hardness values measured on the ring samples lie on the extensions of the disk samples for the corresponding revolutions.

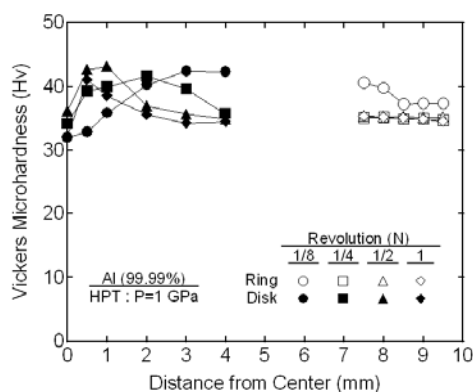


Fig. 3 Microhardness plotted against distance from centers of disk and ring samples for Al.

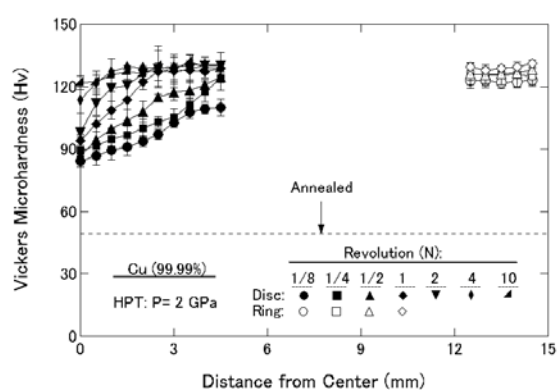


Fig. 4 Microhardness plotted against distance from centers of disk and ring samples for Cu.

All hardness values are plotted as a function of equivalent strain in Figs 5 and 6 for Al and Cu, respectively. Here, the equivalent strain is given as  $\varepsilon = (r\theta/t)/\sqrt{3}$ , where  $r$  is the distance from the center of disk or ring,  $\theta$  is the rotation angle in radian and  $t$  is the thickness of disk or ring [7]. It is apparent that all data points lie on a single line. However, the behavior with respect to equivalent strain is different between Al and Cu. Whereas for Al, a maximum appears at an equivalent strain of  $\sim 2$ , no such a maximum exists for Cu. The hardness variation reaches a steady-state level where no change in hardness occurs with respect to the imposed strain for both Al and Cu. This steady state begins at the equivalent strain of  $\sim 6$  for Al but the onset of the steady state is  $\sim 15$  for Cu.

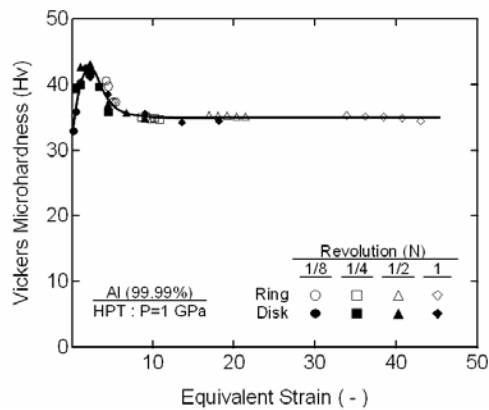


Fig. 5 Microhardness plotted against equivalent strain for all Al data points shown in Fig.3.

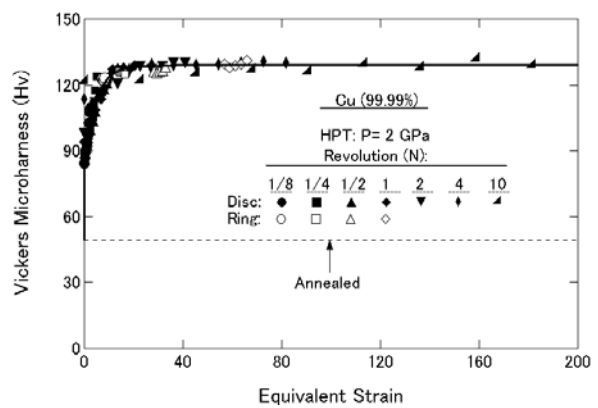


Fig. 6 Microhardness plotted against equivalent strain for all Cu data points shown in Fig.4.

The hardness measurement was carried out along the periphery of the ring samples after revolutions of 1/8, 1/4, 1/2 and 1 under a pressure of 1 and 2 GPa for Al and Cu, respectively. The results are shown in Figs.7 and 8. Most of the hardness values in Al fall on the same level except for the revolution of 1/8. Since the plots in Fig.5 for the 1/8 revolution have not reached the steady-state level, not only the values are higher but also they vary with positions along the periphery. In Cu, the trend is similar to Al so that most of the hardness values lie on a constant level, but close examination reveals that the angular variation is less as the number of the revolution increases. This suggests that the local inhomogeneity is developed when the number of the revolution is small but, as it is increased, the homogeneity is established throughout the ring sample.

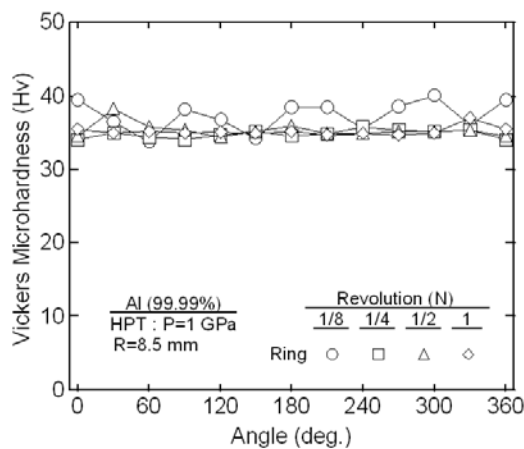


Fig. 7 Microhardness plotted along periphery at middle of Al ring width.

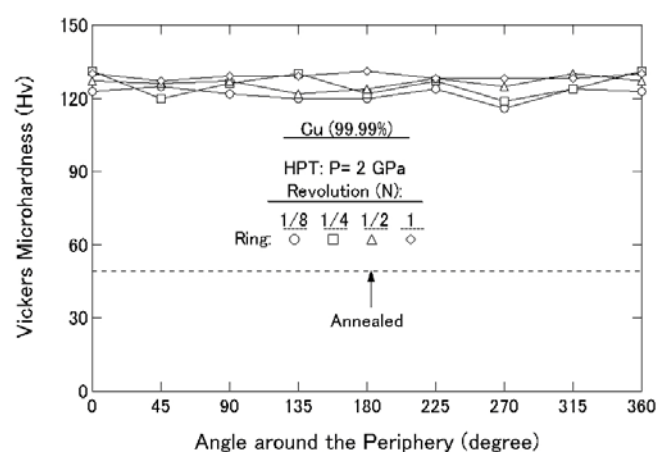


Fig. 8 Microhardness plotted along periphery at middle of Cu ring width.

Figure 9 shows a bright field image (upper) and a dark field image (lower) taken from an Al ring sample subjected to strain corresponding to the hardness maximum. There are grains with irregular configurations of grain boundaries and many dislocation are visible with the grains. A bright field image and dark field image taken from an Al ring sample strained to the steady state are also shown in Fig.10 including an SAED pattern recorded from an area of 6.3  $\mu\text{m}$  in diameter. Here, the dark field image was taken with the diffracted beam indicated by an arrow. The grain size is reduced to  $\sim 1.5 \mu\text{m}$  and there are few dislocations within grains. Most of grain boundaries are smooth and straight despite the fact that the sample was heavily deformed. Such a feature appears to be typical of grains after annealing.

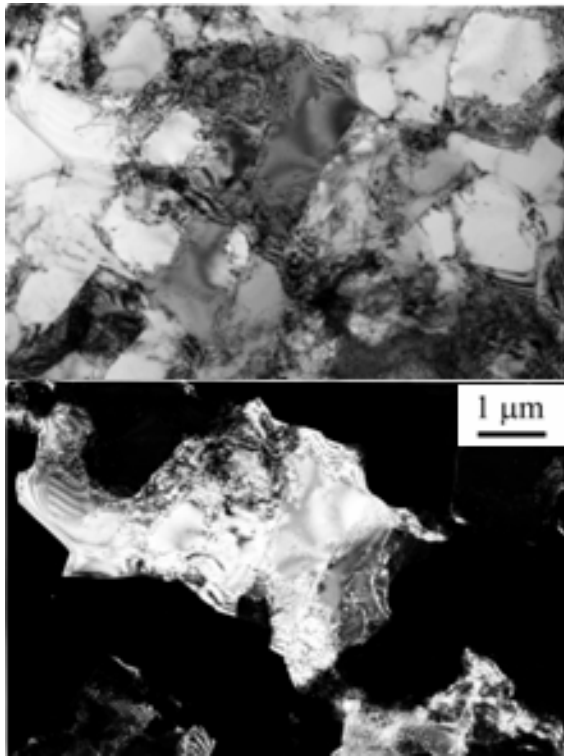


Fig. 9 TEM bright field image (upper) and dark field image (lower) taken from Al ring processed to strain corresponding to hardness maximum. .

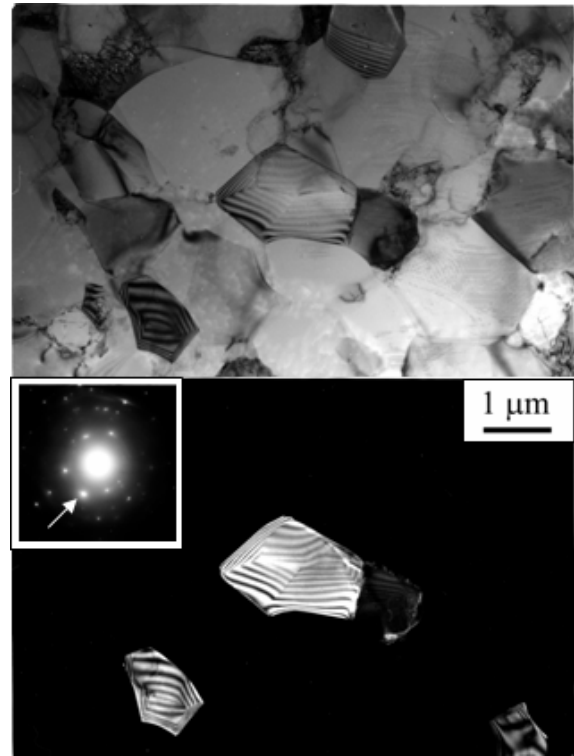


Fig. 10 TEM bright field image (upper) and dark field image (lower) with SAED pattern taken from Al ring processed to strain at steady state.

Microstructures of Cu ring samples are shown in Fig.11 (a) and (b) for the strain well below the onset of the steady state and for the strain well within the steady state, respectively. For the former, the microstructure consists of subgrains with an average size of  $\sim 1 \mu\text{m}$  and because of a net type of the SAED pattern, the boundary misorientation should be very low. Some grains are present where many dislocations are visible. For the latter, some grain boundaries appear to be straight and better defined. Inspection reveals that there are grains with a low density of dislocations as indicated by an arrow whereas some grains contain many dislocations. This suggests that recrystallization may have taken place.

## Discussion

This study has clearly demonstrated that the ring sample is successfully applied not only to Al but also to Cu in the HPT process. The hardness variation was expressed with a unique function of the equivalent strain for both Al and Cu regardless of the use of disk or ring samples. It was shown that the ring sample can produce a homogeneous microstructure throughout the sample in HPT.



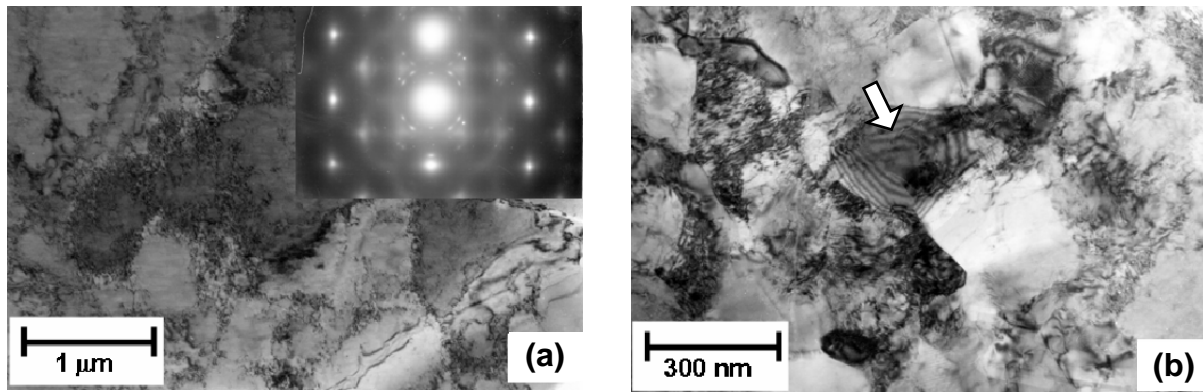


Fig. 11 TEM micrographs of Cu rings strained to (a) well below onset of steady state and to (b) well within steady state.

Analyzing the hardness variation with respect to the equivalent strain, it was shown that Al and Cu exhibit different behavior. Whereas pure Al takes a hardness maximum at an equivalent strain of  $\sim 2$  and enters into a steady state at an equivalent strain of  $\sim 6$ , no maximum appears in pure Cu and the steady state is reached at the equivalent strain of  $\sim 15$ . It is considered that this difference is attributed to the difference in dislocation mobility associated with the difference in stacking fault energy (SFE). Because SFE is large in Al, dislocations are easy to move and annihilate each other. However, SFE of Cu is small so that dislocations tend to accumulate and more strain is stored in the sample. The enhancement of the stored energy initiates recrystallization for new grains which are free from dislocations. Schematic illustration for microstructural evolution along with the hardness variation is illustrated in Figs.12 and 13 for pure Al and pure Cu, respectively.

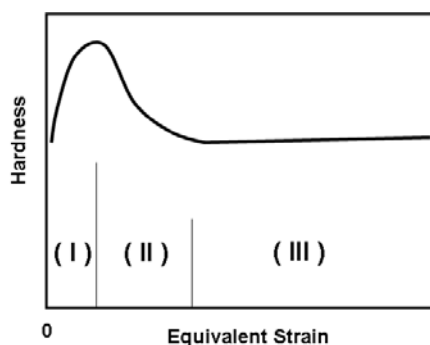
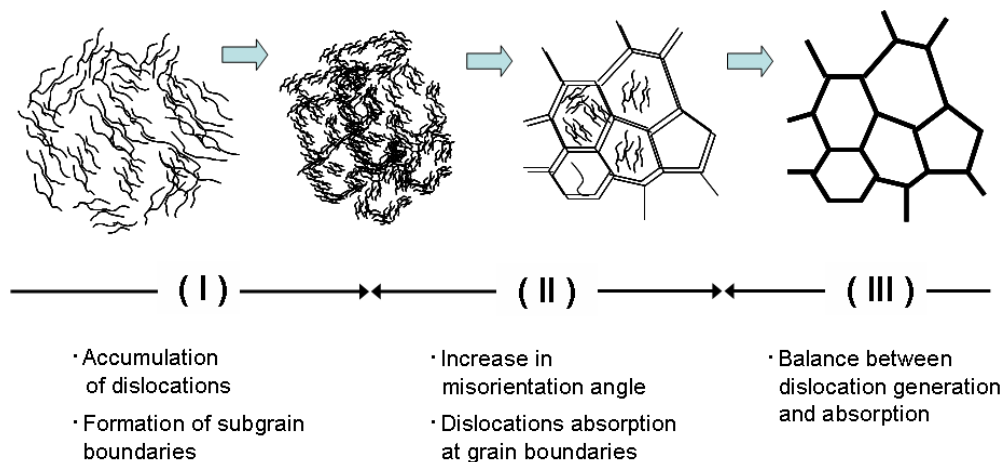


Fig. 12 Schematic illustration of microstructural evolution with straining for grain refinement in pure Al.



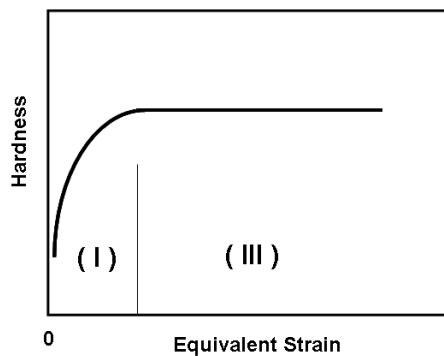
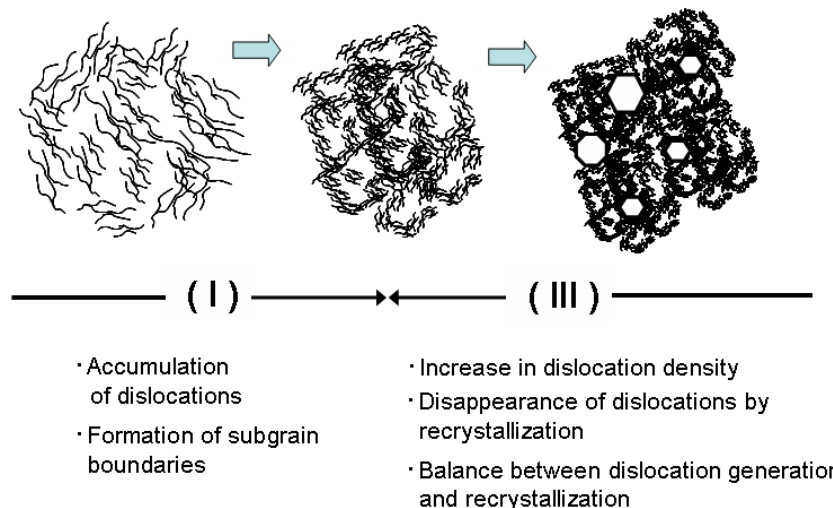


Fig. 13 Schematic illustration of microstructural evolution with straining for grain refinement in pure Cu.



## Conclusions

1. For the HPT process, ring samples are successfully applied not only to pure Al but also to pure Cu. It is then possible to produce homogeneous microstructure throughout the ring samples.
2. The hardness variation for each of Al and Cu is expressed by a unique function of equivalent strain. Whereas pure Al takes a hardness maximum at an equivalent strain of ~2 and enters into steady state at an equivalent strain of ~6, the hardness gradually increases to a steady state at a equivalent strain of ~15 in pure Cu. This difference should be attributed to the difference in stacking fault energy between Al and Cu which leads to the difference in the dislocation mobility.

## Acknowledgements

This study was supported in part by the Light Metals Educational Foundation of Japan and in part by a Grant-in-Aid for Scientific Research from the Ministry of Education, Culture, Sports, Science and Technology, Japan, in the Priority Area "Giant Straining Process for Advanced Materials Containing Ultra-High Density Lattice Defects".

## References

- [1] R.Z. Valiev, Y. Estrin, Z. Horita, T.G. Langdon, M.J. Zehetbauer: Y.T. Zhu: JOM Vol.58 (4) (2006), p. 33.
- [2] G. Sakai, K. Nakamura, Z. Horita, T.G. Langdon : Mater. Sci. Eng. Vol.A406 (2005), p. 268.
- [3] P.W. Bridgman: Studies in Large Plastic Flow and Fracture, McGraw-Hill, New York, NY (1952).
- [4] S. Erbel: Metals Technology, (1979), p.482.
- [5] I. Saunders, J. Nutting: Metal Science Vol.18 (1984), p.571.
- [6] Y. Harai, Y. Ito, Z. Horita: Scripta Mater. Vol.58 (2008), p.469.
- [7] F. Wetscher, A. Vorhauer, R. Stock, R. Pippan: Mater. Sci. Eng. Vol.A387-389 (2004), p. 809.